



HAL
open science

Chaotic dynamics in passively Q-switched Tm:LiYF₄ laser operating at 2.3 μ m on the 3H₄ \rightarrow 3H₅ transition

Hippolyte Dupont, Matthieu Glasset, Pavel Loiko, Patrick Georges, Frédéric Druon

► To cite this version:

Hippolyte Dupont, Matthieu Glasset, Pavel Loiko, Patrick Georges, Frédéric Druon. Chaotic dynamics in passively Q-switched Tm:LiYF₄ laser operating at 2.3 μ m on the 3H₄ \rightarrow 3H₅ transition. *APL Photonics*, 2024, 9 (9), pp.096106. 10.1063/5.0220220 . hal-04723538

HAL Id: hal-04723538

<https://iogs.hal.science/hal-04723538v1>

Submitted on 7 Oct 2024

HAL is a multi-disciplinary open access archive for the deposit and dissemination of scientific research documents, whether they are published or not. The documents may come from teaching and research institutions in France or abroad, or from public or private research centers.

L'archive ouverte pluridisciplinaire **HAL**, est destinée au dépôt et à la diffusion de documents scientifiques de niveau recherche, publiés ou non, émanant des établissements d'enseignement et de recherche français ou étrangers, des laboratoires publics ou privés.

Chaotic dynamics in passively Q-switched Tm:LiYF₄ laser operating at 2.3 μm on the ³H₄ → ³H₅ transition

Hippolyte Dupont,¹ Matthieu Glasset,¹ Pavel Loiko,² Patrick Georges,¹ and Frédéric Druon¹

¹*Université Paris-Saclay, Institut d'Optique Graduate School, CNRS, Laboratoire Charles Fabry, 91127 Palaiseau, France*

²*Centre de Recherche sur les Ions, les Matériaux et la Photonique (CIMAP), UMR 6252 CEA-CNRS-ENSICAEN, Université de Caen Normandie, 6 Boulevard Maréchal Juin, 14050 Caen Cedex 4, France*

(*Electronic mail: frederic.druon@institutoptique.fr)

(Dated: 10 August 2024)

We report on the chaotic dynamics in a passively Q-switched 2.3-m Thulium laser operating on the ³H₄ → ³H₅ transition. The experiment exploits a Tm:LiYF₄ crystal and various laser cavity configurations, involving optional cascade laser on the ³F₄ → ³H₆ transition at 1.9 μm. The saturable absorber employed is Cr²⁺:ZnSe, which is exclusively saturated by the 2.3 μm laser. An analysis of the Q-switched dynamics shows a pronounced inclination of the laser operation towards unstable and chaotic behavior. To understand the origins of this chaos, we monitor the population of the metastable ³F₄ level via cascade laser operation at 1.9 μm, underlying this variable as an interesting parameter to survey chaotic instabilities.

The investigation of lasers operating in the short-wave infrared to mid-infrared spectral ranges is a significant and promising area of research for a variety of specific applications [1]. Among them, wavelengths around 2.3 μm are appealing for gas sensing in the atmosphere, non-invasive glucose blood measurements, and pumping of mid-infrared optical parametric oscillators using non-oxide crystals. The trivalent thulium ions (Tm³⁺) possess an energy-level structure that allows for emission around 2.3 μm through the ³H₄ → ³H₅ transition. They are also well-known for lasers operating at 1.9 μm according to the ³F₄ → ³H₆ transition. Passive Q-switching (PQS) is a well-known approach for generating pulsed output from solid-state lasers. Thulium lasers operating in the PQS regime have been addressed in the previous studies [2-5], and it seems that unstable regimes were often observed, especially when operating at 2.3 μm [7-10]. However, the sensitivity of PQS Tm-lasers to unstable or chaotic regimes has never been precisely analyzed. In the present work, we use classical tools of chaos characterization to clarify the propension of a Tm doped solid state laser to reach deterministic disorder. We demonstrate an intermittency route to chaos observed within a single Q-switched cavity, which is an atypical behavior for Q-switching [11,12]. Indeed, this particular chaotic regime with intermittency appears to be linked to the cascade laser scheme, as indicated by Valcarcel et al. in their work [13]. Furthermore, intermittency routes to chaos have been reported in various laser systems under the influence of external feedback [14-19] or multiple cavity Q-switching [20]. On the other hand, chaotic behavior was observed in a single-cavity Q-switched configuration due to mode competition [3,21-26]. In the latter case, routes to chaos occurred mainly with bifurcation [23-26]. And, to the best of our knowledge, the occurrence of intermittency routes to chaos in a single isolated passively Q-switched laser has never been observed. In the context of this study, the fact that Tm-lasers are prone to intermittent chaotic transitions makes PQS lasers employing Tm³⁺-doped crystals an interesting subject of investigation. Particularly noteworthy is the demonstration that we can monitor - through cascade laser operation at 1.9

μm - the population variation of the metastable ³F₄ level, giving access to another interesting parameter to study chaotic establishment. This paper presents a detailed examination of the dynamic behavior of a PQS Tm-laser operating on the ³H₄ → ³H₅ transition around 2.3 μm. It highlights significant jitter issues at low repetition rates and open ways for investigating the deterministic chaotic dynamics and intermittent routes. The findings contribute to advancing our understanding of the complex behavior of Tm-lasers and have implications for the design and optimization of lasers in the short-wave infrared to mid-infrared ranges for various applications.

The laser set-up is shown in Fig. 1. Two overlapping cavities allowing for operation both at 1.9 μm and 2.3 μm are designed based on the same gain medium, an a-cut 3 at.% Tm:LiYF₄ crystal. It is pumped by a Ti:Sapphire laser emitting up to 2.2 W at 780 nm. The laser resonator is designed to allow an optional cascade laser at 1.9 μm. The saturable absorber (SA) employed is a 1.2-mm-thick, 2.76×10¹⁸ at/cm³-doped Cr²⁺:ZnSe crystal. It is positioned in the cavity arm where it can be exclusively saturated by the 2.3 μm laser. The modulation depth at this wavelength is 4.1%. The cascade laser can be obtained using a dichroic mirror that separates the two laser lines: a “continuous-wave” line at 1.9 μm and a Q-switched line at 2.3 μm. The laser power at 1.9 μm can be adjusted or even blocked using a diaphragm inserted in the 1.9-μm cavity arm. The simple 1.9-μm V-shaped laser cavity naturally operates in the continuous-wave (cw) regime when no laser oscillations at 2.3 μm are imposed. The transmission of the output coupler for the 2.3 μm laser line TOC is 1% or 3%, while for the 1.9 μm laser line, TOC is fixed to 2%.

For the described laser configuration, with or without cascade laser, the Q-switched operation regime at 2.3 μm is obtained with a pulse repetition rate in the range of 1 to 30 kHz and a nearly constant pulse duration of ~4.7 μs (Fig. 1b). The pulse repetition rate increases linearly with the pump power (Fig. 1d). The error bars indicate the root mean square (r.m.s.) deviation of the repetition rate over a few seconds of measurement (quantifying the time jitter). Chaotic zones can be clearly identified when the dispersion of the repetition rate ex-

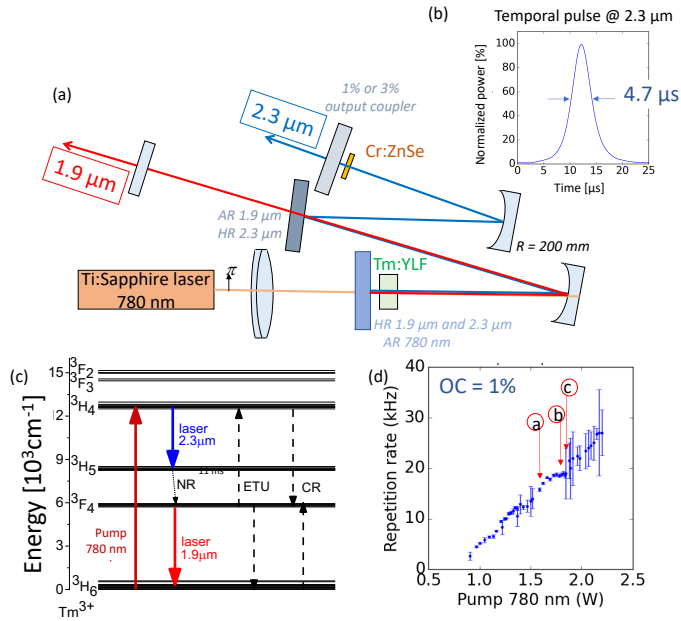


FIG. 1. Tm:YLF laser passively Q-switched by a Cr:ZnSe saturable absorber: (a) laser setup; (b) a typical oscilloscope trace of a single Q-switched pulse; (c) the energy-level scheme of Tm³⁺ ions showing the observed laser transitions; (d) pulse repetition rate vs. pump power, with or without cascade laser for a 1% output coupling at 2.3 μm ; the error bars represent the r.m.s. of the pulse repetition rate measurements.

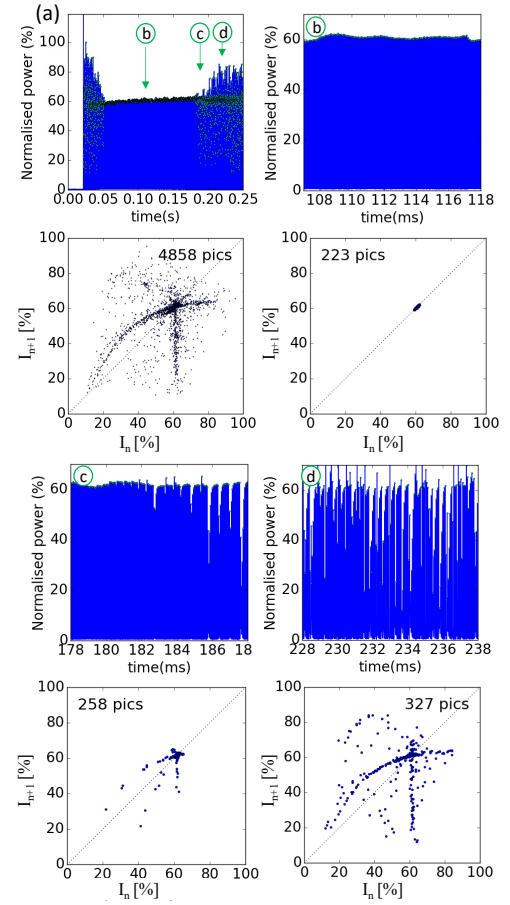


FIG. 3. Temporal transition regime at 2 W of pump power from transitory stable regime to chaos. (b,c,d) are temporal zooms of the oscillogram (a), the second line indicates the corresponding Poincaré maps of the peak intensities $I_{n+1} = f(I_n)$.

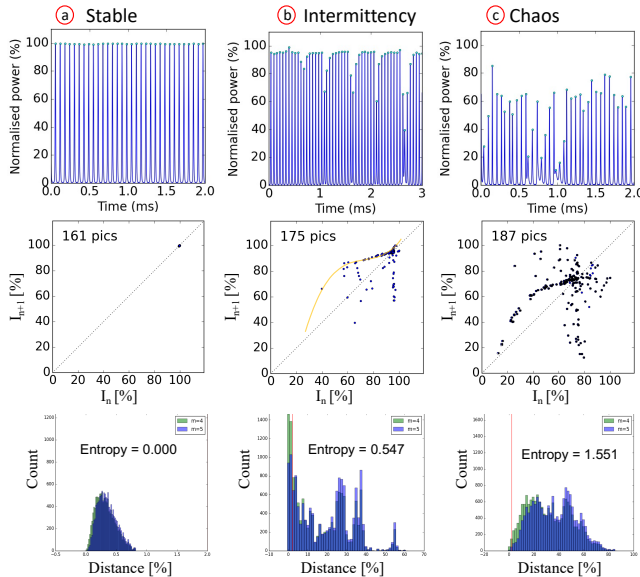


FIG. 2. (a-c) Various characteristic regimes: the first line represents the oscilloscope traces of laser emission at 2.3 μm , the second one shows the Poincaré maps of the Q-switched peaks $I_{n+1} = f(I_n)$ and the third line presents histograms used for calculating the peak entropy (embedded dimension $m = 4$ and 5). Three dynamic regimes are presented: 1st column: a single-pulse stable regime, 2nd column: intermittency regime, 3rd column: chaotic regime. A cubic fit is plotted for the laminar phase in the case of intermittencies.

plodes [26]. On the other hand, stable zones are clearly visible with a relatively low jitter. The stable zones vary with the different laser configurations. With the 1% output coupler at 2.3 μm , they are within the ranges of 8.9 – 10.9 kHz and 13.2 – 16 kHz in the absence of cascade laser, and within 9.5 – 12.3 kHz and 14.6 – 19.4 kHz with cascade laser. The cascade laser is useful for visualizing chaos by using the 1.9 μm laser as an additional output parameter. This raises the question of whether the chaotic regime remains equivalent without the cascade laser, specifically by blocking the 1.9 μm laser emission. The answer is yes: in this scenario, we observe the same chaotic dynamics with identical intermittency structures. The chaotic behaviors are equivalent and the route to chaos always involves the same type of intermittencies.

We are now going to focus our study on the dynamics involved in the route to chaos. For a precise analysis of the temporal behavior of the PQS Tm-laser, we use a large-buffer (up to 134 Mpts) oscilloscope allowing for long-time acqui-

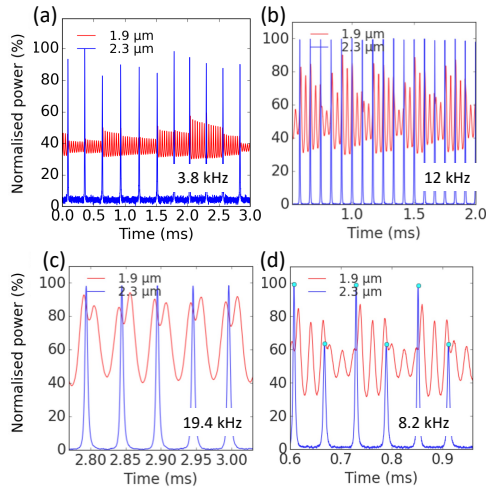


FIG. 4. Simultaneous monitoring of temporal dynamics of 1.9 μm and 2.3 μm emissions from the cascade Tm:YLF laser at different repetition rates: 2.3-μm passively Q-switched laser (in blue) and 1.9-μm “cw” laser (in red). For different repetition rates.

sition without sampling aliasing and an accurate peak-power detection. We will focus on the transition regime from stable Q-switching to a chaotic regime which occurs around a repetition rate of 20 kHz (Fig. 1d). For this analysis, we extract from the oscillograms the pulse peak powers. This allows us to access in interesting parameters for the study of chaos such as sample entropy and Poincaré maps. To analyze different regimes, we plot in Fig. 2 the oscillograms in the first line, and the corresponding Poincaré maps of peak intensity in the second line indicating the entropy of the peak intensity. Increasing the pump power, we start from a stable regime (Fig. 2a) with null entropy and subsequently observe the transitional phase with intermittencies (Fig. 2 b with an intermediate entropy of 0.547) before reaching chaotic instabilities (Fig. 2c, with an entropy of 1.551). This intermittency regime (in the Pomeau–Manneville scenario[27–28]) appears as long periods of almost regular behavior –called laminar phases– interrupted by short glitches.

On the Poincaré maps plotting the functions $I_{n+1} = f(I_n)$ –where I_n is the intensity of the n-th laser pulse– during the laminar phase, a characteristic pattern above the bisector line appears in the intermittency regime, the pattern that even extends in the chaotic regime. This pattern seems to be very similar to the one observed in the type I intermittency scenario as in reference [28] page 254. It is then possible to fit the peaks of the laminar phase evolution $I_{n+1} = f(I_n)$, with a polynomial (cubic, in our case) function allowing one to estimate that the Poincaré curve tangentially approaches the bisector line with a distance ε of 0.0168. To go further, it is also possible to evaluate the exponential dependence between the length of the laminar phase L and ε . In our case the measured average laminar phase was about 7 to 8 pulse periods ($\langle L \rangle = 7.75$), and we find $L = \varepsilon^{-\lambda}$, with $\lambda = 0.501$, being close to the theoretical one of 1/2 which tends to confirm the type I intermittency hypothesis. A similar route to chaos also appears in transitory

regimes. In Fig. 3, we observe such transition for the cavity employing TOC = 1% at 2.3 μm at 2 W of pump power. In this experiment, the laser cavity at 2.3 μm is mechanically unblocked and the pulse train is monitored during a quarter of second. Before reaching the chaotic regime, a stable pulse train is observed at a repetition rate of 20 kHz corresponding to the one expected, cf. Fig. 1(d), for this pump power. However, this stable regime is not accessible in the steady-state regime. With this pulse train, it is possible to evaluate the Lyapunov coefficient: during the stable regime (Fig. 3b) its value is around 0.05 and it reaches 0.15 and 0.18 for the chaotic and intermittency regimes. When the laser emission at 2.3 μm appears, the absorption changes in the Cr:ZnSe absorber. We measured its temperature elevation to be around 26 °C using a thermal camera (and considering an emissivity of 0.05 [31]). With no surprise, for chaotic systems, this slight evolution of the temperature –whose characteristic time is about 1 s– indicates that very small changes on the saturable absorption parameters can drastically change the final regime of laser operation transiting from stable to chaotic behavior through intermittencies.

To go further, we want to show that 1.9 μm laser can help to understand the Q-switched operation instability issues[32]. For this, we monitor both the 2.3 μm and 1.9 μm lasers simultaneously. Since the metastable ³F₄ manifold is the upper laser level of the 1.9 μm laser transition, Fig. 1(c), we can access its population variation under cascade laser operation. This can be done in a kind of perturbative regime giving access to an important underlying parameter (namely, the population of the intermediate long-living Tm³⁺ state, ³F₄) that will help us to understand the instability issues linked to the ³H₄ → ³H₅ and ³F₄ → ³H₆ cascade transitions of Tm³⁺ ions. At low pulse repetition rates (typically below 5 kHz), the dispersion in the repetition rate is small but the Q-switched regime appears unstable (Fig. 4a). Indeed, at such repetition rates, the relaxation oscillation of the 1.9 μm (such as the ³F₄ population) relaxes between two subsequent Q-switched pulses at 2.3 μm and the 1.9 μm laser oscillates several times with a repetition rate around 20 kHz without synchronization with the Q-switched pulse train. This irregular relaxation periods are visible via the 1.9-μm laser (with 7 to 9 oscillations, for example at 3.8 kHz). Each 2.3 μm pulse then starts with a different population state leading to the instability. However, at higher pump powers (and, accordingly, higher pulse repetition rates for the 2.3 μm laser emission), it is possible to find stable Q-switching regimes, where both 2.3 μm and 1.9 μm laser emissions are periodically synchronized (Fig. 4b,c). A similar effect is also observed in the case of periodic-stable regime, Fig. 4d,g.

By simultaneously accessing the temporal behavior of the 2.3-μm and 1.9-μm lasers, we are able to explore comparatively their sensitivity. Figure 5 represents these concomitant recordings for a stable Q-switched regime and isolated intermittencies. It is noticeable that the laser intensity at 1.9 μm (related to the underlying ³F₄ level population) appears more unstable than the Q-switched pulse train at 2.3 μm. For example, in the stable regime, the variation can be observed on the 1.9-μm laser power without any impact on the pulse train

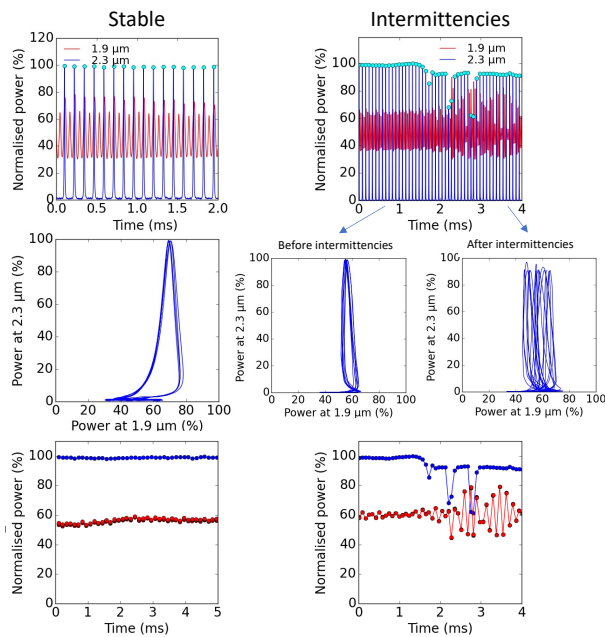


FIG. 5. Simultaneous monitoring of temporal dynamics of 1.9 μm and 2.3 μm emissions from the cascade Tm:YLF laser: 2.3- μm passively Q-switched laser (in blue) and 1.9- μm “cw” laser (in red). For different regimes stable and with intermittencies. First line: oscillograms of laser emissions. Second line: corresponding phase diagrams obtained by plotting the 2.3 μm laser power versus that at 1.9 μm . Third line: the corresponding normalized intensities of single Q-switched peaks at 2.3 μm and the peak power at 1.9 μm at the beginning of each 2.3- μm laser pulse (measured at 20% intensity level on the pulse rise) versus time. This analysis allows for visualizing the difference of sensitivities between the 2.3 μm and 1.9 μm lasers.

stability at 2.3 μm . Even more representative, after an isolated intermittency whereas the Q-switched operation regime comes back instantly to a stable regime, the 1.9- μm laser remains unstable. This is also visible on the phase diagrams obtained by plotting the laser power at 2.3 μm vs. that at 1.9 μm as shown in the third line of Fig. 4: the obtained curves are clearly more spread along the abscissa axis (i.e., the 1.9- μm laser power). Having access to such original phase diagrams is practical for studying operation regimes of cascade lasers, in particular, from the point of view of studying intermittencies with a clear observation of multiple loops. The dual-wavelength cascade laser represents an attractive atypical tool to look at the premises of chaos monitoring. Currently, theoretical modelling using the basic coupled non-linear rate equations is not sufficient to explain chaotic behavior and intermittencies. Finding relevant additional equations (thermal or multi-modal) seems to be required to achieve a more reliable modelling, however finding the correct additional coupled parameters is quite challenging and need to be confirmed experimentally.

In conclusion, we investigated the dynamic behavior of a passively Q-switched Tm-laser at 2.3 μm . For this study we used a Ti:Sapphire pumping which may appears not optimal for an industrial system -compared to laser-diode pumping for

example-, however, its high brightness allows a better control for the spatial single-mode operation, which is crucial to simplify the study of the chaotic behavior. The findings reveal a tendency to exhibit chaotic operation. The cascade lasers at 2.3 μm and 1.9 μm are then identified as interesting variables for monitoring laser instability dynamics. We observed, in stable regimes, a synchronization process between the two cascade lasers: the Q-switched laser repetition rate at 2.3 μm and the relaxation oscillations of the 1.9 μm laser. This is the first time for our best knowledge that a cascade laser has been used to study chaotic behavior. This novel utilization presents an interesting, original and powerful tool for understanding complex laser dynamics. The research demonstrates that Tm³⁺-based laser systems are prone to intermittency route to chaos, which is an exceptional characteristic for passively Q-switched lasers. Moreover, transition regimes show that a temporary stable regime can occur before reaching the chaotic one. The proposed setup uses a slow saturable absorber and no mode-locking operation has been observed. Nevertheless, beside chaotic regimes in Q-switch, dynamics in mode-locked regime using a fast saturable absorber could be also interesting to investigate in Tm-doped lasers operating at 2.3 μm . Overall, this research contributes to understanding the dynamic behavior of Q-switched Tm lasers and sheds light on the underlying factors leading to unstable and chaotic regimes of laser operation with implications for optimizing MIR lasers that often involve cascade laser transitions.

¹A. Godard, C. R. Phys. **8**(10), 1100 (2007).

²R. Faoro, M. Kadankov, D. Parisi, S. Veronesi, M. Tonelli, V. Petrov, U. Griebner, M. Segura, and X. Mateos, Opt. Lett. **37**, 1517–1519 (2012).

³B. Yao, Y. Tian, G. Li, and Y. Wang, Opt. Express **18**, 13574–13579 (2010).

⁴Y. Du, B. Yao, X. Duan, Z. Cui, Y. Ding, Y. Ju, and Z. Shen, Opt. Express **21**, 26506–26512 (2013).

⁵M. Segura, M. Kadankov, X. Mateos, M. C. Pujol, J. J. Carvajal, M. Aguiló, F. Díaz, U. Griebner, and V. Petrov, Opt. Express **20**, 3394–3400 (2012).

⁶F. Canbaz, I. Yorulmaz, and A. Sennaroglu, Opt. Lett. **42**, 1656–1659 (2017).

⁷S. Wang, H. Huang, H. Chen, X. Liu, S. Liu, J. Xu, and D. Shen, OSA Continuum **2**, 1676–1682 (2019).

⁸H. Huang, S. Wang, H. Chen, O. L. Antipov, S. S. Balabanov, and D. Shen, Opt. Express **27**, 38593–38601 (2019).

⁹H. Zhang, J. He, Z. Wang, J. Hou, B. Zhang, R. Zhao, K. Han, K. Yang, H. Nie, and X. Sun, Opt. Mater. Express **6**, 2328–2335 (2016).

¹⁰E. Kifle, P. Loiko, L. Guillemot, J.-L. Doualan, F. Starecki, A. Braud, A. Hèideur, and P. Camy, Optics Communications **500**, 127219 (2021).

¹¹D. Y. Tang, S. P. Ng, L. J. Qin, and X. L. Meng, Opt. Lett. **28**, 325–327 (2003).

¹²C. Bonazzola, J. Opt. Soc. Am. B **38**, 1398–1404 (2021).

¹³G. J. de Valcárcel, E. Roldán, V. Espinosa, and R. Vilaseca, Physics Letters A **206**, 359–364 (1995).

¹⁴C.-M. Kim, K.-S. Lee, J. M. Kim, S.-O. Kwon, C.-J. Kim, and J.-M. Lee, J. Opt. Soc. Am. B **10**, 1651–1654 (1993).

¹⁵E. Villafana-Rauda, R. Chiu, M. Mora-Gonzalez, F. Casillas-Rodriguez, C. Medel-Ruiz, and R. Sevilla-Escoboza, Results in Physics **12**, 908–913 (2019).

¹⁶G. Martel, M. Bennoud, B. Ortac, T. Chartier, J.-M. Nunzi, G. Boudebs, and F. Sanchez, Journal of Modern Optics **51**, 85–95 (2004).

¹⁷C. Letellier, M. Bennoud, and G. Martel, Chaos, Solitons Fractals **33**, 782–794 (2007).

¹⁸D. Mgharaz and M. Brunel, J. Opt. Soc. Am. B **36**, 2184–2192 (2019).

¹⁹G. U. Kim, H. T. Choo, D. I. Kim, Y.-J. Park, S.-H. Gong, and C.-M. Kim, J. Opt. Soc. Am. B **20**, 302–306 (2003).

²⁰H. Huang, J. He, B. Zhang, K. Yang, C. Zuo, J. Xu, X. Dong, and S. Zhao, Appl. Phys. B **96**, 815–820 (2009).

- ²¹C. Jauregui, C. Stihler, and J. Limpert, *Adv. Opt. Photon.* **12**, 429–484 (2020).
- ²²H. W. Mocker and R. J. Collins, *Applied Physics Letters* **7**, 270–273 (1965).
- ²³Q. Zhang, B. Feng, D. Zhang, P. Fu, Z. Zhang, Z. Zhao, P. Deng, J. Xu, X. Xu, Y. Wang, and X. Ma, *Phys. Rev. A* **69**, 053815 (2004).
- ²⁴M. Larotonda, A. Yacomotti, and O. Martinez, *Optics Communications* **169**, 149–158 (1999).
- ²⁵C. Bracikowski and R. Roy, *Chaos: An Interdisciplinary Journal of Nonlinear Science* **1**, 49–64 (1991).
- ²⁶M. Kovalsky and A. Hnilo, *Opt. Lett.* **35**, 3498–3500 (2010).
- ²⁷P. M. Y. Pomeau, *Commun.Math. Phys.* **74**, 189–197 (1980).
- ²⁸C. V. Pierre Bergé, Yves Pomeau, *L'ordre dans le chaos: Vers une approche déterministe de la turbulence* (Collection : "Enseignement des sciences", Hermann Edition, 1997).
- ²⁹D. Y. Tang, M. Y. Li, and C. O. Weiss, *Phys. Rev. A* **46**, 676–678 (1992).
- ³⁰"The intermittency route to chaos," in *Deterministic Chaos* (John Wiley Sons, Ltd, 2005) Chap. 5, pp. 69–88, <https://onlinelibrary.wiley.com/doi/pdf/10.1002/3527604804.ch5>.
- ³¹X. Zhang, S. Zhao, Q. Wang, Q. Zhang, L. Sun, and S. Zhang, *IEEE Journal of Quantum Electronics* **33**, 2286–2294 (1997).
- ³²H. Dupont, L. Guillemot, P. Loiko, R. M. Solé, X. Mateos, M. Aguiló, F. Díaz, A. Braud, P. Camy, P. Georges, and F. Druon, *Opt. Express* **31**, 34201–34212 (2023).